# The chromosomal passenger complex and centralspindlin independently contribute to contractile ring assembly

Lindsay Lewellyn,[1] Ana Carvalho,[1] Arshad Desai,[1] Amy S. Maddox,[2] and Karen Oegema[1]

[1]Department of Cellular and Molecular Medicine, Biomedical Sciences Graduate Program, Ludwig Institute for Cancer Research, University of California, San Diego, La Jolla, CA 92093
[2]Department of Pathology and Cell Biology, Institute for Research in Immunology and Cancer, University of Montréal, Montréal, Quebec H3C 3J7, Canada

The chromosomal passenger complex (CPC) and centralspindlin are conserved cytokinesis regulators that localize to the spindle midzone, which forms between the separating chromosomes. Previous work placed the CPC and centralspindlin in a linear pathway that governs midzone formation. Using *Caenorhabditis elegans* embryos, we test whether there is a similar linear relationship between centralspindlin and the CPC in contractile ring constriction during cytokinesis. We show that simultaneous inhibition of the CPC kinase Aurora B$^{AIR-2}$ and the centralspindlin component MKLP1$^{ZEN-4}$ causes an additive constriction defect. Consistent with distinct roles for the proteins, inhibition of filamentous septin guanosine triphosphatases alleviates constriction defects in Aurora B$^{AIR-2}$–inhibited embryos, whereas inhibition of Rac does so in MKLP1$^{ZEN-4}$-inhibited embryos. Centralspindlin and the CPC are not required to enrich ring proteins at the cell equator but instead regulate formation of a compact mature ring. Therefore, in contrast to the linear midzone assembly pathway, centralspindlin and the CPC make independent contributions to control transformation of the sheet-like equatorial band into a ribbon-like contractile ring at the furrow tip.

## Introduction

In animal cells, cytokinesis is accomplished by constriction of a contractile ring that forms around the cell equator between the segregating chromosomes. The structural components of the contractile ring include three interconnected filament systems: actin filaments, bipolar filaments of the motor myosin II, and septin filaments. The septins are a membrane-associated filament system that binds and is recruited to the ring by anillin, a filament cross-linker that also binds directly to actin and activated myosin II (Weirich et al., 2008; D'Avino, 2009; Zhang and Maddox, 2010). During constriction, myosin filaments are proposed to use their motor activity to move along actin filaments, shortening the ring in a fashion analogous to muscle contraction (Schroeder, 1975). However, in contrast to muscle, the ring is progressively disassembled as it constricts (Schroeder, 1972; Carvalho et al., 2009).

To ensure the spatial and temporal coupling of cytokinesis with chromosome segregation, contractile ring assembly is directed by signals from the anaphase spindle (D'Avino et al., 2005; Glotzer, 2005; Eggert et al., 2006; von Dassow, 2009). Contractile ring assembly and constriction are coordinately controlled by signals from the centrosomal microtubule asters and spindle midzone, a set of microtubule bundles that forms between the separating chromosomes. The microtubule bundles in the midzone serve as a scaffold that recruits cytokinesis-signaling molecules (Glotzer, 2005; Eggert et al., 2006). Stable bundling of midzone microtubules requires three components: (1) the chromosomal passenger complex (CPC), (2) the centralspindlin complex, and (3) the microtubule-binding/cross-linking protein Ase1/PRC1$^{SPD-1}$. Centralspindlin is a heterotetramer (Pavicic-Kaltenbrunner et al., 2007) composed of two molecules of the kinesin-6, MKLP1$^{ZEN-4}$, and two molecules of MgcRacGAP$^{CYK-4}$,

Correspondence to Karen Oegema: koegema@ucsd.edu

Abbreviations used in this paper: CPC, chromosomal passenger complex; dsRNA, double-stranded RNA; GAP, GTPase-activating protein; IP, immunoprecipitation; MRLC, myosin II regulatory light chain; NEBD, nuclear envelope breakdown.



The Rockefeller University Press $30.00
J. Cell Biol. Vol. 193 No. 1 155–169
www.jcb.org/cgi/doi/10.1083/jcb.201008138

which contains a GTPase-activating protein (GAP) domain for Rho family GTPases. The CPC is a four-protein complex composed of the mitotic kinase Aurora B$^{AIR-2}$ and three additional subunits (INCENP$^{ICP-1}$, Survivin$^{BIR-2}$, and Borealin$^{CSC-1}$) that localize and activate the kinase (Ruchaud et al., 2007; Carmena et al., 2009). Although centralspindlin, the CPC, and PRC1$^{SPD-1}$ are all required to form stable midzone microtubule bundles, their relative contributions to cytokinesis differ. Inhibition of PRC1$^{SPD-1}$ in *Caenorhabditis elegans* or in human cells does not prevent contractile ring assembly or constriction (Verbrugghe and White, 2004; Mollinari et al., 2005), whereas inhibition of either centralspindlin (Glotzer, 2005; Eggert et al., 2006) or the CPC (Carmena, 2008) causes a marked constriction defect. In *C. elegans*, ring constriction kinetics in PRC1$^{SPD-1}$-depleted embryos are similar to those in controls, and the first cytokinesis completes successfully (Verbrugghe and White, 2004; Lewellyn et al., 2010). In contrast, inhibition of centralspindlin or the CPC leads to a two- to threefold reduction in constriction rate and cytokinesis failure (Powers et al., 1998; Raich et al., 1998; Schumacher et al., 1998; Jantsch-Plunger et al., 2000; Kaitna et al., 2000; Severson et al., 2000; Speliotes et al., 2000; Canman et al., 2008; Lewellyn et al., 2010). The less severe effect of PRC1$^{SPD-1}$ depletion could be a result of the fact that the CPC, and to a lesser extent centralspindlin, still targets to the microtubules between the separating chromosomes in the absence of PRC1$^{SPD-1}$-mediated bundling (Kurasawa et al., 2004; Verbrugghe and White, 2004; Mollinari et al., 2005; Lewellyn et al., 2010). Alternatively, it is possible that midzone targeting is not essential for the contribution of the CPC and centralspindlin to contractile ring constriction (Mollinari et al., 2005; Cesario et al., 2006; Nishimura and Yonemura, 2006; Verbrugghe and White, 2007).

Two roles in contractile ring assembly/constriction have been proposed for centralspindlin. In human cells, the MgcRacGAP$^{CYK-4}$ subunit of centralspindlin has been shown to serve as an anchoring site for the polo-kinase–dependent targeting of the RhoGEF, Ect2 (Yüce et al., 2005; Zhao and Fang, 2005; Chalamalasetty et al., 2006; Kamijo et al., 2006; Nishimura and Yonemura, 2006; Brennan et al., 2007; Burkard et al., 2007; Petronczki et al., 2007), which has been proposed to locally activate Rho at the cell equator. The second proposed role of centralspindlin centers on its GAP activity. *C. elegans* embryos expressing MgcRacGAP$^{CYK-4}$ with mutations predicted to disrupt its GAP activity, but which do not alter midzone assembly, exhibit a constriction defect that mimics centralspindlin loss of function. Depletion of the Rac homologue CED-10 can rescue the completion of constriction in the GAP mutant embryos, suggesting that Rac is the target GTPase inhibited by the centralspindlin GAP activity (Canman et al., 2008). The importance of the GAP activity and the idea that it targets Rac are also supported by evidence from *Drosophila melanogaster* and vertebrate cells (D'Avino et al., 2004; Yoshizaki et al., 2004; Zavortink et al., 2005). The centralspindlin GAP activity was also shown to be critical for cytokinesis in *Xenopus laevis* embryos; however, in this case, the target was proposed to be Rho rather than Rac (Miller and Bement, 2009). Thus, although there is agreement on the importance of the GAP activity for constriction, the identity of the target remains controversial (D'Avino and Glover, 2009; Glotzer, 2009).

The CPC localizes to chromosomes during prophase and then transitions to midzone microtubules in anaphase. Although the Aurora B targets that mediate its role in constriction are not known, it has been proposed that the CPC contributes to cytokinesis by targeting and/or activating centralspindlin (Kaitna et al., 2000; Severson et al., 2000; Giet and Glover, 2001; Hauf et al., 2003; Minoshima et al., 2003; Verbrugghe and White, 2004; Guse et al., 2005; Zhu et al., 2005). Recently, a mechanism has been proposed in which centralspindlin is constitutively phosphorylated on a conserved site (S710 in human MKLP1) that causes it to bind 14-3-3, which sequesters it and prevents it from stably targeting to the midzone. Phosphorylation by the CPC on an adjacent conserved site (S708 in human MKLP1) releases centralspindlin from 14-3-3 and allows it to cluster and accumulate at the midzone (Douglas et al., 2010). In *C. elegans*, genetic evidence, combined with the observation that inhibition of centralspindlin or the CPC leads to similar constriction defects, led to the proposal that the CPC is upstream of centralspindlin in a linear pathway (Severson et al., 2000).

Here, we test whether the dependency of centralspindlin on the CPC for midzone targeting translates into a similar linear pathway during their regulation of ring constriction. We show that simultaneous inhibition of Aurora B$^{AIR-2}$ and the centralspindlin component MKLP1$^{ZEN-4}$ leads to an additive constriction defect compared with either inhibition alone. In addition, distinct perturbations alleviate the constriction defects in centralspindlin and CPC-inhibited embryos. Thus, although centralspindlin depends on the CPC for midzone targeting, the two complexes make independent contributions to ring constriction. We pinpoint the step requiring centralspindlin and the CPC, showing that they are not required for the initial accumulation of contractile ring proteins in an equatorial band but instead regulate the structural transformation that converts the sheet-like equatorial band into a ribbon-like contractile ring at the furrow tip.

## Results

### Simultaneous inhibition of Aurora B$^{AIR-2}$ and MKLP1$^{ZEN-4}$ leads to an additive defect in contractile ring constriction

During the first embryonic division of *C. elegans*, inhibition of centralspindlin or the CPC by mutation or depletion leads to a two- to threefold reduction in the constriction rate compared with controls. In addition, after constricting to ~50% of their starting diameter, the contractile rings open back up and cytokinesis fails (Fig. 1, A–E; Canman et al., 2008; Lewellyn et al., 2010). The similar magnitude of the constriction rate decrease in Aurora B$^{AIR-2}$– and MKLP1$^{ZEN-4}$-depleted embryos is consistent with the idea that the dependency of centralspindlin on the CPC for targeting to the midzone (Severson et al., 2000; Douglas et al., 2010) translates into a similar relationship in the regulation of constriction. For simplicity, and because of the availability of fast-acting, temperature-sensitive mutants (Severson et al., 2000), we focused on inhibition of Aurora B$^{AIR-2}$ and the

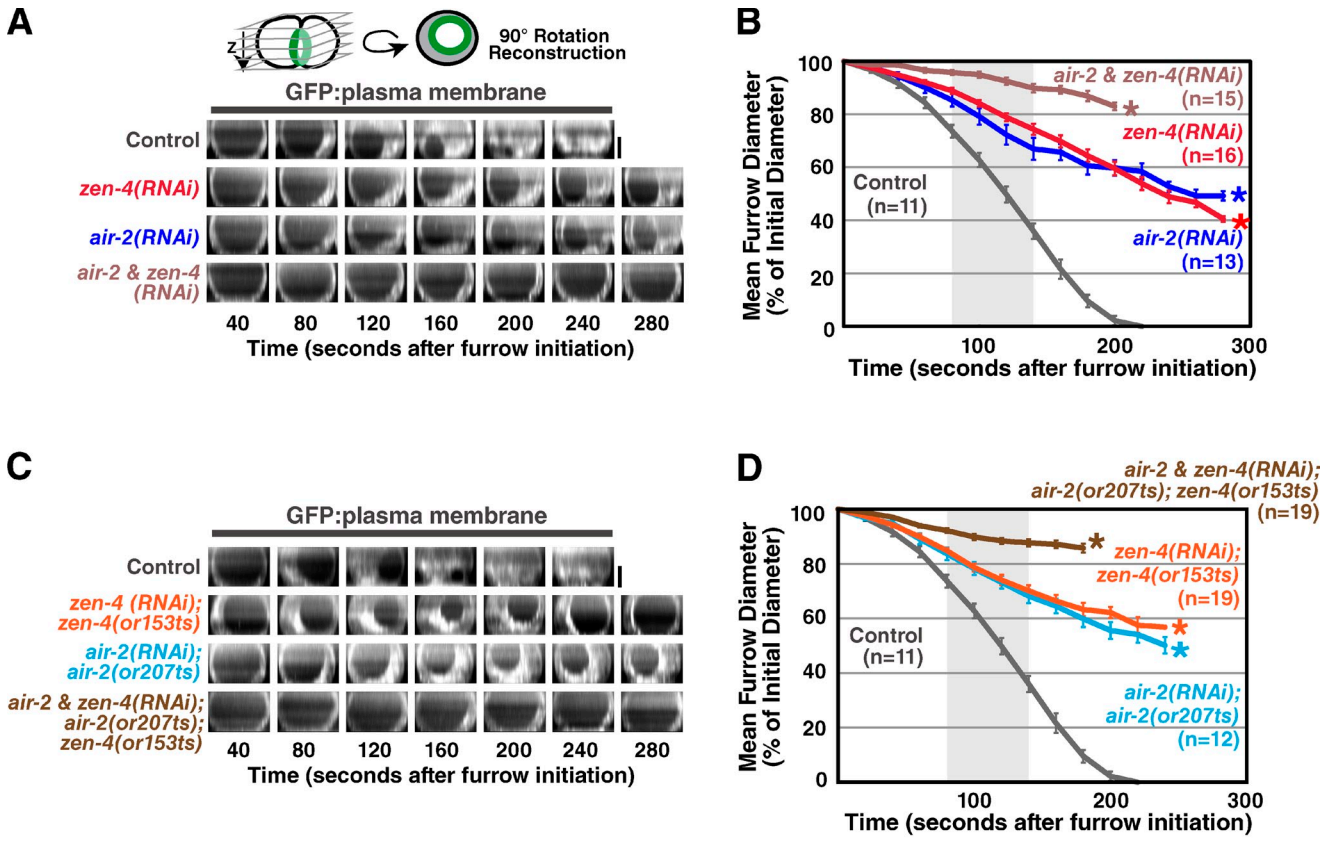


Figure 1. **Simultaneous inhibition of centralspindlin and the CPC leads to an additive defect in contractile ring constriction.** (A and C) End-on reconstructions of the division plane were generated as indicated in the schematic during cytokinesis in control, *zen-4(RNAi)*, *air-2(RNAi)*, and *air-2 & zen-4(RNAi)* embryos (A) or in control, *zen-4(RNAi);zen-4(or153ts)*, *air-2(RNAi);air-2(or207ts)*, and *air-2 & zen-4(RNAi);air-2(or207ts);zen-4(or153ts)* embryos (C) overexpressing a GFP plasma membrane marker. (B and D) Mean furrow diameter measured from end-on reconstructions is plotted versus time for the conditions in A (B) and C (D). Embryos were removed from the mean when the furrow began to regress. The asterisks indicate the point when fewer than two embryos still had ingressing furrows. The control curve in B and D is the same. (E) The mean maximum extent of ingression expressed as a percentage of initial diameter (left) and the mean rate of diameter decrease over the time interval 80–140 s after constriction onset (right) are shown for the indicated conditions. The asterisks indicate significant differences relative to *zen-4(RNAi);zen-4(or153ts)* (two-tailed *t* test, $P < 0.05$). Error bars are SEM. For consistency, all imaging in this figure was done by shifting worms to the restrictive temperature (26.5°C) 30–60 min before dissection of embryos from the mothers so that embryos were at the restrictive temperature during the entire interval between fertilization and the end of cytokinesis. Bars, 10 µm.

centralspindlin component MKLP-1$^{ZEN-4}$. However, an essentially identical reduction in constriction rate is also observed after inhibition of the centralspindlin component CYK-4 (Canman et al., 2008) or inhibition of the other three CPC components (Fig. 1 E and not depicted). If the CPC contributes to furrow ingression exclusively by promoting the activation/targeting of centralspindlin, simultaneous depletion of centralspindlin and the CPC should result in a constriction defect similar to that resulting from inhibition of either complex alone. In contrast, embryos codepleted of Aurora B$^{AIR-2}$ and MKLP1$^{ZEN-4}$ exhibited an additive constriction defect, constricting at less than half the rate of embryos depleted of Aurora B$^{AIR-2}$ or MKLP1$^{ZEN-4}$ alone and completing only ∼20% of ingression before regressing, compared with ∼50% for the single depletions (Fig. 1, B, D, and E; and Video 1). Quantitative Western blotting confirmed that MKLP1$^{ZEN-4}$ and Aurora B$^{AIR-2}$ were ∼95% depleted and that the extent of depletion was the same for both proteins in the single- and double-depleted embryos (Fig. S1).

To ensure that we were completely inhibiting both proteins, we combined RNAi-mediated depletion with fast-acting, temperature-sensitive mutations that allowed us to use temperature upshift to rapidly inactivate residual protein remaining after RNAi. We used two previously characterized alleles, *zen-4(or153ts)* and *air-2(or207ts)*, that allow rapid inactivation of MKLP1$^{ZEN-4}$ and Aurora B$^{AIR-2}$, respectively, upon temperature upshift (*or153ts* and *or207ts* result in a D520N substitution in MKLP1$^{ZEN-4}$ and a P265L substitution in the Aurora B kinase domain, respectively; Severson et al., 2000; Pavicic-Kaltenbrunner et al., 2007). The constriction defects in *zen-4(or153ts)* or *air-2(or207ts)* embryos that were depleted of MKLP1$^{ZEN-4}$ or Aurora B$^{AIR-2}$ and upshifted before fertilization to inactivate residual protein was the same as that after MKLP1$^{ZEN-4}$ or Aurora B$^{AIR-2}$ depletion alone, indicating that the RNAi leads to a complete loss of function in constriction. Double mutant embryos codepleted of Aurora B$^{AIR-2}$ and MKLP1$^{ZEN-4}$ and then upshifted before fertilization exhibited an additive constriction defect essentially identical to that resulting from the double depletion alone (Fig. 1, B, D, and E; and Video 2). We also obtained the same additive phenotype upon double depletion of the CPC component CSC-1 (the *C. elegans* homologue of borealin; Romano et al., 2003; Gassmann et al., 2004) and MKLP1$^{ZEN-4}$ (Fig. 1 E). We conclude that centralspindlin and the CPC make independent contributions to contractile ring constriction.

## Postmeiotic inhibition of Aurora B$^{AIR-2}$ enhances the constriction defect resulting from MKLP1$^{ZEN-4}$ depletion

A complication in analyzing CPC depletions is its role in the segregation of the oocyte-derived chromosomes, which undergo two rounds of meiotic segregation after fertilization to generate the two polar bodies (Fig. 2 A). Both rounds of meiotic chromosome segregation and polar body extrusion fail in CPC-inhibited embryos, generating an oocyte-derived pronucleus that contains four times the normal amount of DNA (Fig. 2 B; Kaitna et al., 2000; Rogers et al., 2002). Thus, the enhanced cytokinesis defect resulting from depleting Aurora B$^{AIR-2}$ or CSC-1 along with MKLP1$^{ZEN-4}$ may arise from this excess of poorly structured DNA on the mitotic spindle. To specifically assess the mitotic role of the CPC, we upshifted *air-2(or207ts)* embryos to inactivate Aurora B$^{AIR-2}$ after meiosis was complete (Fig. 2, A–D; and Video 3). Postmeiotic upshift resulted in a constriction defect that was qualitatively similar, but slightly less severe, than Aurora B$^{AIR-2}$ depletion, an approximately twofold decrease in constriction rate relative to similarly shifted control embryos, and regression after 60% of constriction was completed (Fig. 3, A and C).

To determine whether postmeiotic inhibition of Aurora B$^{AIR-2}$ would enhance the effect of MKLP1$^{ZEN-4}$ depletion on contractile ring constriction, we depleted MKLP1$^{ZEN-4}$ in the *air-2(or207ts)* mutant embryos and upshifted them after meiosis. Postmeiotic inactivation of Aurora B$^{AIR-2}$ reduced both the rate and maximum extent of constriction in MKLP1$^{ZEN-4}$-depleted embryos an additional twofold (0.039 µm/s and 21.6% constriction completed in MKLP1$^{ZEN-4}$-depleted embryos with postmeiotic Aurora B$^{AIR-2}$ inactivation vs. 0.073 µm/s and 42.3% constriction completed in MKLP1$^{ZEN-4}$-depleted embryos; Fig. 3, A and C). We conclude that Aurora B$^{AIR-2}$ inhibition enhances the effect of MKLP1$^{ZEN-4}$ depletion on contractile ring constriction, even if the meiotic chromosome segregation function of Aurora B$^{AIR-2}$ is properly executed.

## Disrupting mitotic chromosome segregation or midzone microtubule bundling does not enhance the effect of MKLP1$^{ZEN-4}$ depletion on contractile ring constriction

Postmeiotic Aurora B$^{AIR-2}$ inactivation still leads to the presence of anaphase chromatin bridges and to a reduction in the density of the midzone microtubule bundles (Fig. 2 D; Severson et al., 2000). Therefore, we tested whether either of these consequences of CPC disruption contributed to the additive constriction defect observed in MKLP1$^{ZEN-4}$- and Aurora B$^{AIR-2}$–inhibited embryos. Embryos codepleted of MKLP1$^{ZEN-4}$ and CENP-C$^{HCP-4}$, an inner kinetochore component required for chromosome segregation, exhibited very similar constriction kinetics to embryos depleted of MKLP1$^{ZEN-4}$ alone (Fig. 3, B and C). Embryos codepleted of MKLP1$^{ZEN-4}$ and PRC1$^{SPD-1}$, a microtubule-binding protein required to form stable midzone microtubule bundles (Verbrugghe and White, 2004), also exhibited constriction kinetics essentially identical to embryos depleted of MKLP1$^{ZEN-4}$ alone, as did *zen-4(or153ts)* mutant embryos depleted of both CENP-C$^{HCP-4}$ and PRC1$^{SPD-1}$ (Fig. 3, B and C). Depletion of PRC1$^{SPD-1}$ and MKLP1$^{ZEN-4}$ or codepletion of PRC1$^{SPD-1}$ and MKLP1$^{ZEN-4}$ also did not prevent the localization of Aurora B$^{AIR-2}$ to microtubules extending into the region between the separated chromosomes (Fig. 3 D and Video 4; Lewellyn et al., 2010). We conclude that the additive ring constriction phenotype observed after simultaneous inhibition of Aurora B$^{AIR-2}$ and MKLP1$^{ZEN-4}$ cannot be explained by the involvement of Aurora B$^{AIR-2}$ in chromosome segregation or midzone microtubule bundling. Cumulatively, these results suggest that Aurora B$^{AIR-2}$ has a role in contractile ring constriction that is independent of its roles in chromosome segregation, MKLP1$^{ZEN-4}$ targeting to the midzone, and midzone microtubule bundling.

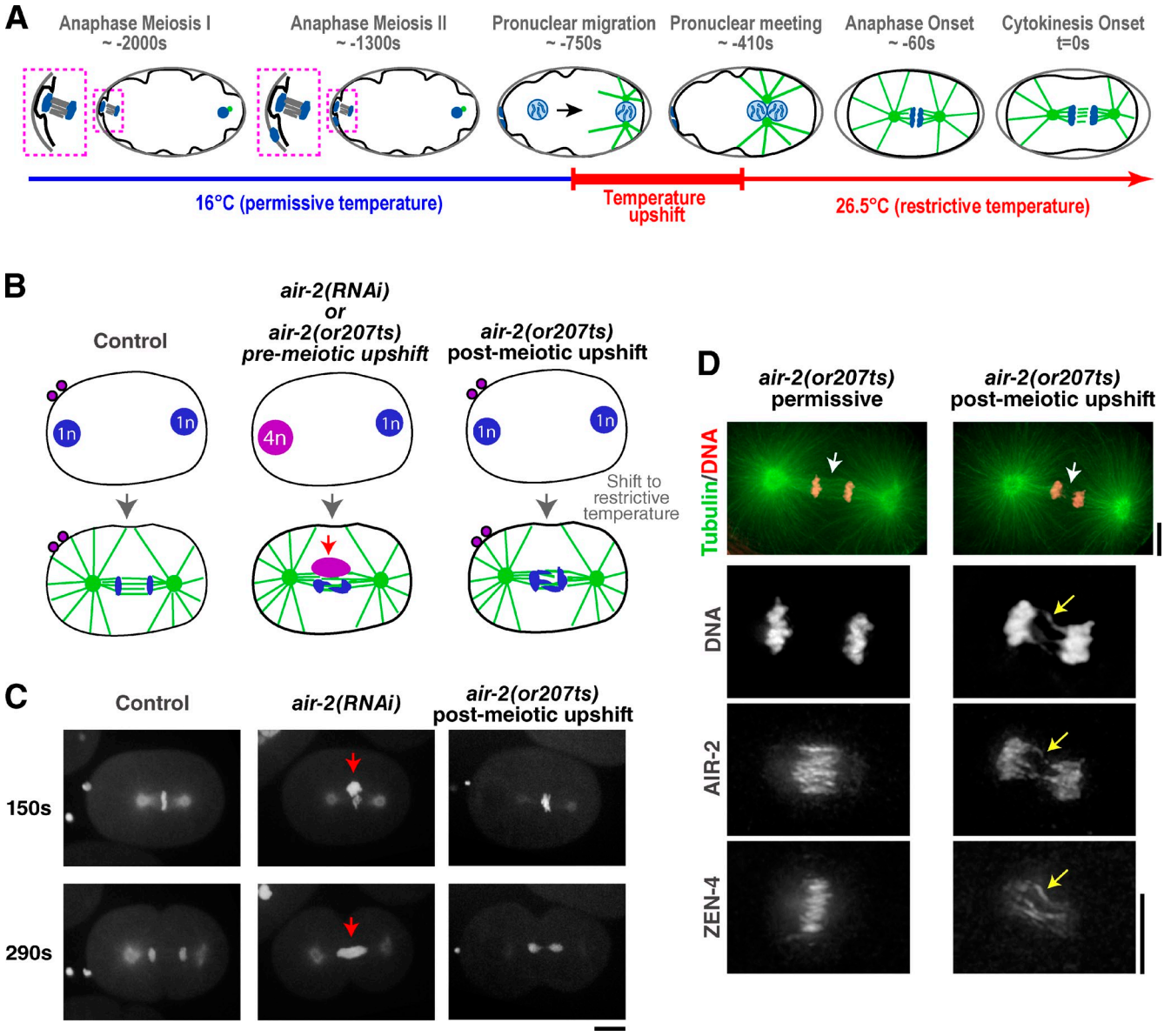


Figure 2. **Postmeiotic upshift of a temperature-sensitive Aurora B$^{AIR-2}$ mutant can be used to bypass the meiotic defects resulting from CPC inhibition.** (A) Schematic illustrating the postmeiotic upshift conditions. Embryos are maintained at the permissive temperature (16°C) after fertilization until both rounds of meiotic chromosome segregation are complete. Embryos are upshifted to the nonpermissive temperature (26.5°C) during migration of the resulting maternal pronucleus toward the sperm pronucleus, which occurs during a ~350-s interval that precedes nuclear envelope breakdown (NEBD), mitosis, and cytokinesis. (B) Schematic showing that *air-2(RNAi)* embryos or *air-2(or207ts)* mutant embryos upshifted before meiosis fail to segregate their chromosomes during the two meiotic divisions, resulting in a maternal pronucleus that contains four times the normal amount of DNA. *air-2(or207ts)* mutant embryos upshifted after meiosis have a normal amount of DNA in the maternal pronucleus. (C) Maximum intensity projections of 5 × 2–µm z series of embryos expressing GFP:tubulin and GFP:histone H2B. Time is given in seconds after NEBD. All embryos were imaged at the restrictive temperature for the mutant. The maternal chromatin resulting from meiotic failure in the *air-2(RNAi)* embryo is indicated (red arrows). Bar, 10 µm. (D) Immunofluorescence of *air-2(or207ts)* embryos fixed at the permissive or restrictive temperature. Images are maximum intensity projections of the midzone region of the cell. At the permissive temperature, the mutant Aurora B$^{AIR-2}$ (P265L) localized to midzone microtubule bundles like the wild-type protein, whereas at the restrictive temperature, Aurora B$^{AIR-2}$ P265L remained on the chromosomes. A few strands of Aurora B$^{AIR-2}$ P265L were observed in the midzone in the anaphase embryos at the restrictive temperature, but closer inspection revealed that these strands corresponded to Aurora B$^{AIR-2}$ P265L localized along chromatin bridges that extended into the region between the chromatin masses (yellow arrows; Severson et al., 2000). Consistent with prior work, the density of midzone microtubules was reduced in the upshifted embryos (white arrows; Severson et al., 2000). In addition, the levels of midzone-localized MKLP1$^{ZEN-4}$ were significantly reduced, and its localization was less focused than that in mutant embryos fixed at the permissive temperature. Bars, 5 µm.

### Depletion of Rac$^{CED-10}$ alleviates the constriction defect resulting from inhibition of MKLP1$^{ZEN-4}$ but not Aurora B$^{AIR-2}$

Recent work has suggested that a key function of centralspindlin is to inactivate the small GTPase Rac (D'Avino and Glover, 2009). Depletion of Rac$^{CED-10}$ alone leads to a slight delay in cytokinesis completion (Fig. 4, A and B, gray lines; Canman et al., 2008), but cytokinesis is always successful. As expected based on prior work (Canman et al., 2008), Rac$^{CED-10}$ depletion led to a significant increase in the maximum extent of constriction in upshifted *zen-4(or153ts)* mutant embryos (mean maximum ingression of 81 ± 11% in Rac$^{CED-10}$-depleted *zen-4(or153ts)*

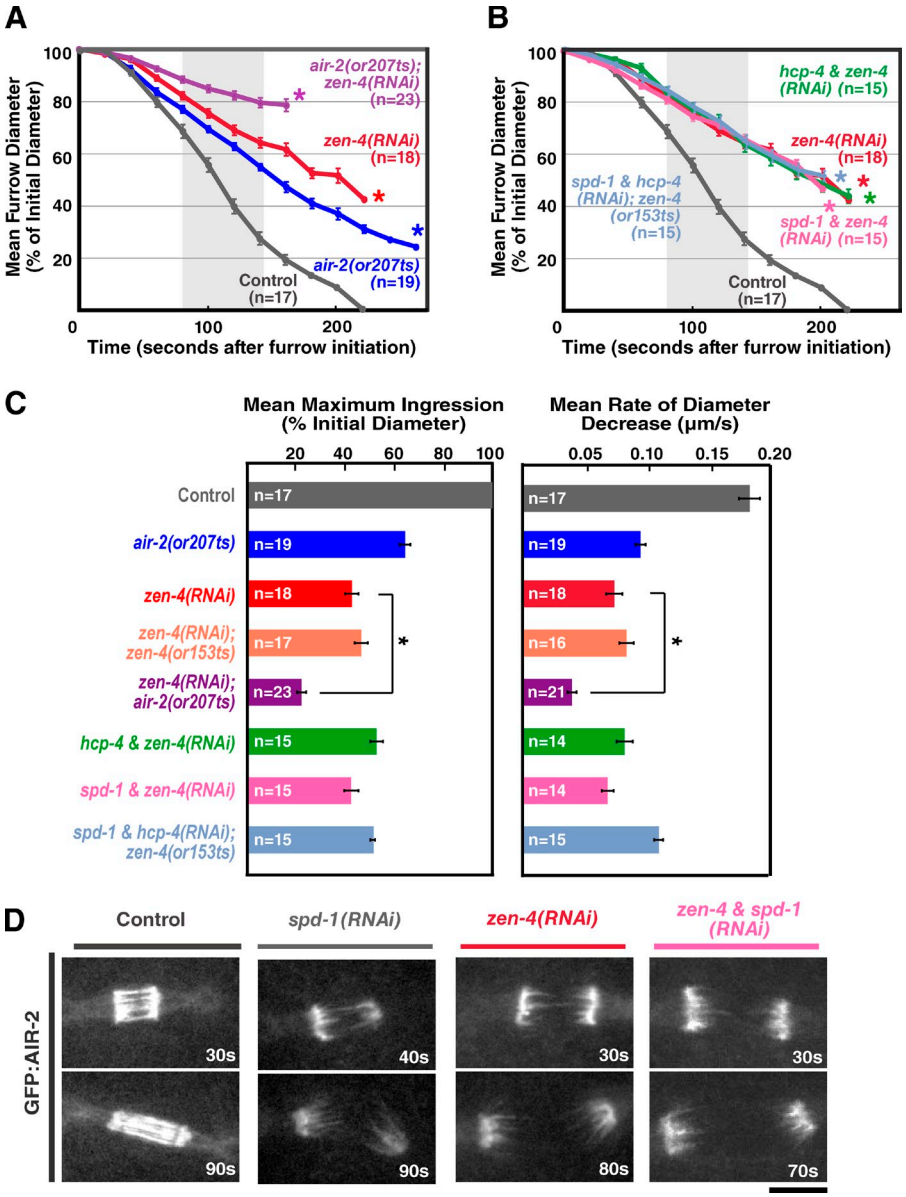


Figure 3. **Aurora B$^{AIR-2}$ has a role in contractile ring constriction that is independent of its roles in meiotic and mitotic chromosome segregation, MKLP1$^{ZEN-4}$ targeting to the midzone, and midzone microtubule bundling.** (A and B) Mean furrow diameter is plotted versus time. Embryos were removed from the mean when the furrow began to regress in that embryo. The asterisks indicate the point when fewer than two embryos still had ingressing furrows. The control curve is the same in A and B. (C) The mean maximum extent of ingression expressed as a percentage of initial diameter (left) and the mean rate of diameter decrease over the time interval 80–140 s after constriction onset (right) are shown for the indicated conditions. The asterisks indicate that mean values for *zen-4(RNAi);air-2(or207ts)* are significantly different (two-tailed *t* test, $P < 0.05$) from *zen-4(RNAi)*. All imaging for A–C was done using the postmeiotic upshift conditions outlined in Fig. 2 A. Error bars are SEM. (D) Single-plane confocal images from time-lapse sequences of control ($n > 20$), *spd-1(RNAi)* ($n = 17$), *zen-4(RNAi)* ($n = 4$), and *zen-4 & spd-1(RNAi)* ($n = 4$) embryos expressing GFP:AIR-2. Bar, 5 µm.

embryos vs. 50 ± 10% for *zen-4(or153ts)* alone; errors are SEM; Fig. 4 A). In contrast, Rac$^{CED-10}$ depletion did not significantly alter the mean extent of constriction in upshifted *air-2(or207ts)* embryos (69 ± 14% vs. 60 ± 12% for the mutant alone; Fig. 4 B). These results support the idea that Aurora B$^{AIR-2}$ makes a contribution to contractile ring constriction that is independent of centralspindlin and suggest that Aurora B$^{AIR-2}$ does not promote constriction by inactivating Rac.

### Aurora B$^{AIR-2}$ does not regulate phosphorylation of the myosin II regulatory light chain (MRLC)

One potential Aurora B target is the MRLC. Vertebrate Aurora B has been shown to phosphorylate MRLC on Ser19 in vitro (Murata-Hori et al., 2000), and phosphorylation of MRLC on Thr18/Ser19 increases the affinity of myosin II for actin and, consequently, its ATPase activity (Sellers et al., 1981, 1985). Rho kinase$^{LET-502}$ is a Rho effector that promotes MRLC phosphorylation by directly phosphorylating MRLC on Ser19 and by inactivating myosin phosphatase, which removes the activating MRLC phosphorylation (Fig. 4 C; Matsumura, 2005). In *C. elegans* embryos, inhibition of the positive regulator of MRLC phosphorylation, Rho kinase$^{LET-502}$, reduces the constriction rate approximately twofold but does not prevent completion of the first division (Fig. 4 D; Piekny and Mains, 2002; Maddox et al., 2007). Conversely, inhibiting the negative regulator of MRLC phosphorylation, myosin phosphatase, by depletion of its myosin-binding subunit MEL-11 leads to a slight increase in the constriction rate (Fig. 4 D; Piekny and Mains, 2002). Simultaneous inhibition of MEL-11 partially rescues the reduced constriction rate in Rho kinase$^{LET-502}$–inhibited embryos (Fig. 4 D; Piekny and Mains, 2002). If Aurora B$^{AIR-2}$ were driving constriction via direct MRLC phosphorylation or via myosin phosphatase inactivation, MEL-11 depletion should likewise alleviate the constriction rate defect in Aurora B$^{AIR-2}$ mutant embryos. However, depletion of MEL-11 in the *air-2(or207ts)* background did not significantly affect the rate or extent of constriction (Fig. 4 D),

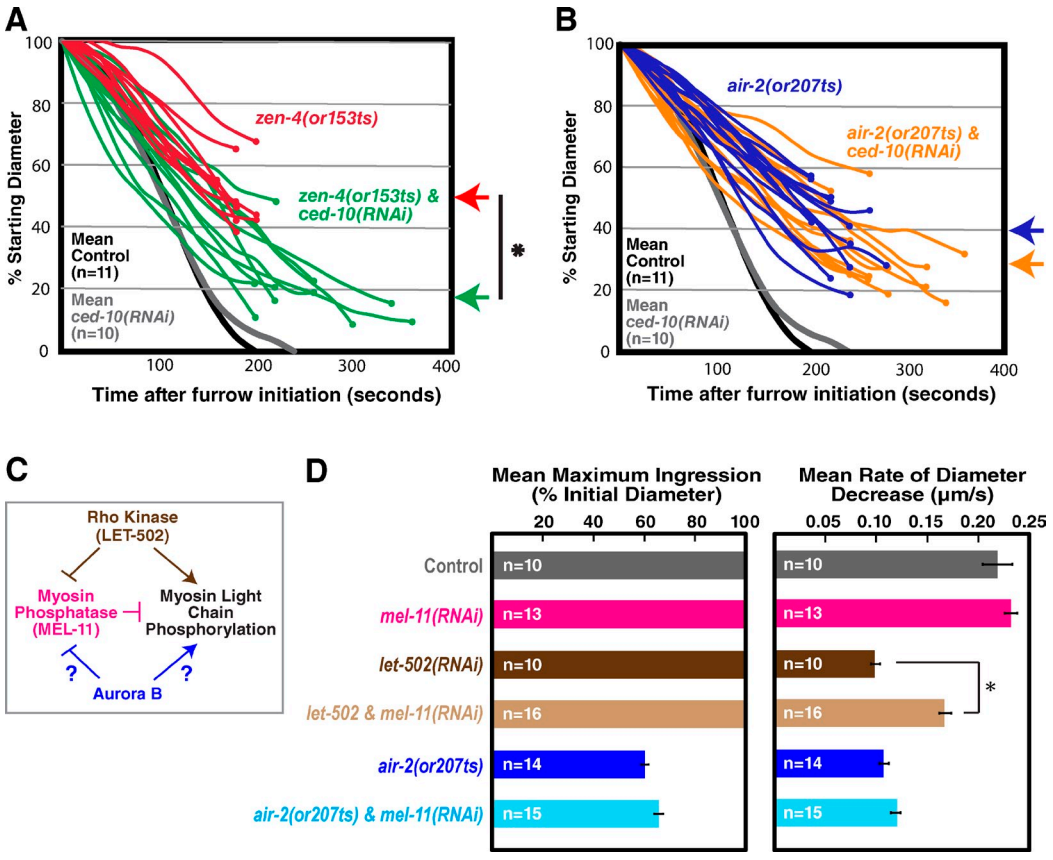


Figure 4. **Depletion of Rac$^{CED-10}$ or the myosin phosphatase subunit MEL-11 does not alleviate the constriction defect resulting from inhibition of Aurora B$^{AIR-2}$.** (A and B) Traces of furrow diameter versus time for individual *zen-4(or153ts)* and *zen-4(or153ts);ced-10(RNAi)* embryos (A) or *air-2(or207ts)* and *air-2(or207ts);ced-10(RNAi)* embryos (B). Furrow diameters were measured in end-on projections of 11-plane z series collected every 20 s. Traces were smoothed by applying a three-point rolling mean. Circles mark the final diameter before regression. Arrows to the right of the graphs mark the mean maximum extent of ingression for each condition. For comparison, mean diameter is plotted versus time for control and *ced-10(RNAi)* embryos. The asterisk indicates that the mean extent of contractile ring constriction in *zen-4(or153ts);ced-10(RNAi)* embryos is significantly greater than that in *zen-4(or153ts)* embryos (two-tailed *t* test, $P < 0.05$). (C) A schematic illustrating the proposed role of Rho kinase$^{LET-502}$ in promoting myosin activation. Potential roles for Aurora B$^{AIR-2}$ are indicated. (D) The mean maximum extent of ingression expressed as a percentage of initial diameter (left) and the mean rate of diameter decrease over the time interval 80–140 s after constriction onset (right) are shown for the indicated conditions. MEL-11 depletion alleviates the reduced constriction rate defect, resulting from inhibition of Rho kinase (LET-502) but not from inhibition of Aurora B$^{AIR-2}$. Error bars are SEM. The asterisk indicates that constriction is significantly faster in *let-502 & mel-11(RNAi)* embryos than in *let-502(RNAi)* embryos (two-tailed *t* test, $P < 0.05$). All imaging was done using the postmeiotic upshift conditions outlined in Fig. 2 A.

making it unlikely that the CPC plays a critical role in promoting MRLC phosphorylation. Consistent with this conclusion, a phosphoproteomic study analyzing the role of Aurora B during mitosis and cytokinesis did not reveal a reduction in MRLC phosphorylation when Aurora B was inhibited (Ozlü et al., 2010).

### Depletion of septin$^{UNC-59}$ alleviates the constriction defect resulting from inhibition of Aurora B$^{AIR-2}$ but not MKLP1$^{ZEN-4}$

The septins are a membrane-associated filament system that binds and is recruited to the contractile ring by anillin (Weirich et al., 2008; D'Avino, 2009; Zhang and Maddox, 2010). Inhibition of either the septins or anillin leads to a similar effect on contractile ring constriction; during the first embryonic cytokinesis, the constriction kinetics are similar to wild type, but the geometry of constriction is altered, and the ring closes symmetrically, rather than asymmetrically, within the division plane (Video 5; Maddox et al., 2007). In septin-depleted embryos, the ring is more susceptible to partial inhibition of contractility, suggesting that it is less robust (Maddox et al., 2007). We depleted septin$^{UNC-59}$ in upshifted *air-2(or207ts)* mutant embryos, expecting to enhance their constriction defect. In contrast, we found that septin$^{UNC-59}$ depletion significantly increased the mean maximum extent of constriction, allowing ~30% (5/17) of the mutant embryos to complete the first division (Fig. 5, B and C; and Video 6). This rescue was specific to the Aurora B$^{AIR-2}$ mutant because septin$^{UNC-59}$ depletion slightly enhanced the constriction defect of upshifted *zen-4(or153ts)* mutant embryos (Fig. 5, A and C; and Video 7) and was unable to rescue the constriction defect when *zen-4* and *air-2* were both inhibited (*zen-4&unc-59(RNAi);air-2(or207ts)*; mean maximum ingression of 17 ± 2%). Very similar results were obtained after partial depletion of anillin$^{ANI-1}$ in the upshifted *air-2(or207ts)* and *zen-4(or153ts)* mutants (Fig. S2). Because septin/anillin inhibition makes the contractile ring less robust, we wondered whether compromising the contractile ring via another means might show a similar differential rescue of

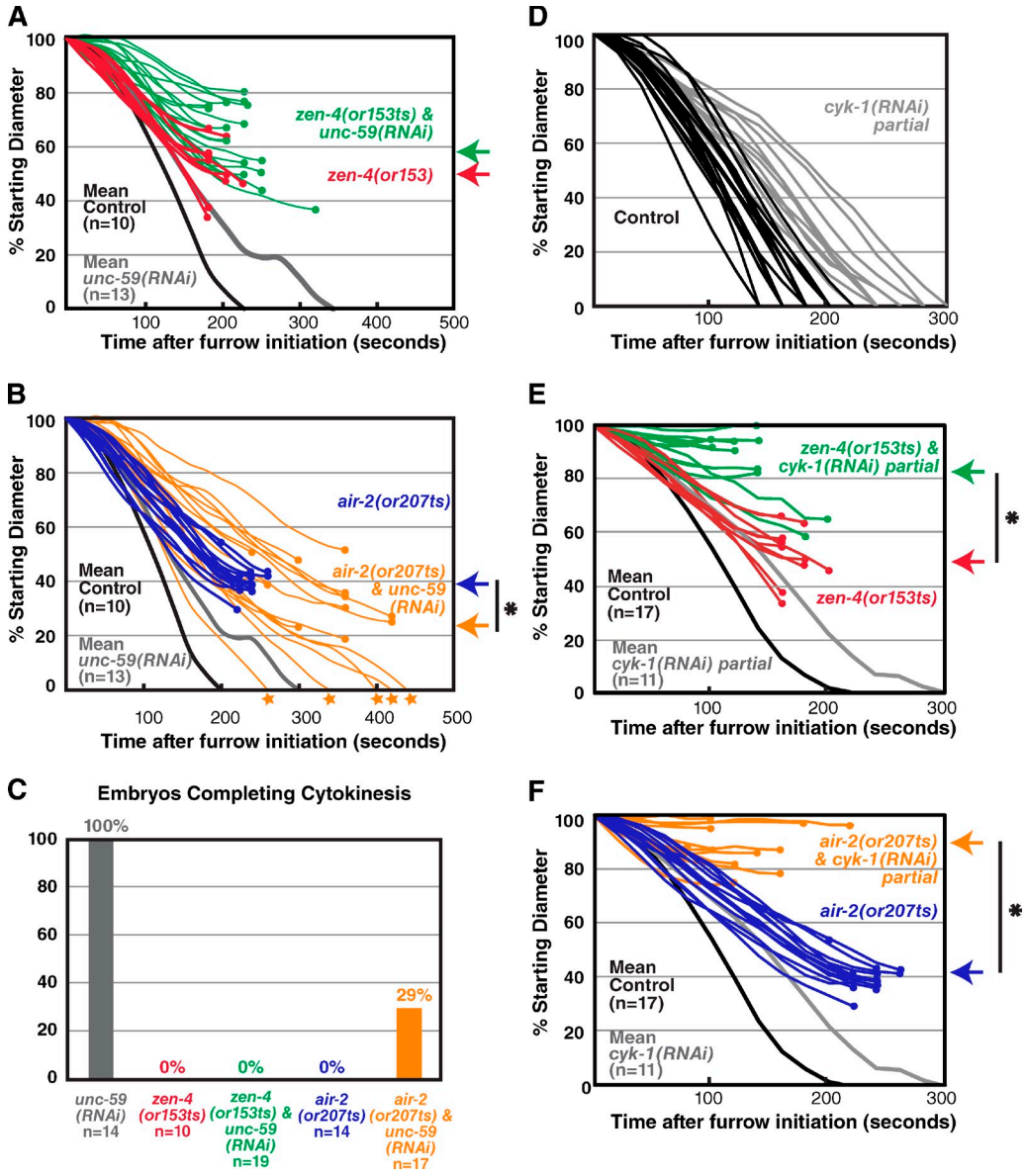


Figure 5. **The contractile ring constriction defect in Aurora B$^{AIR-2}$– but not MKLP1$^{ZEN-4}$-inhibited embryos is alleviated by septin$^{UNC-59}$ depletion.** (A and B) Traces of furrow diameter versus time for individual *zen-4(or153ts)* and *zen-4(or153ts) & unc-59(RNAi)* embryos (A) or *air-2(207ts)* and *air-2(207ts) & unc-59(RNAi)* embryos (B). For comparison, mean contractile ring diameter is plotted versus time for *unc-59(RNAi)* and control embryos. The set of 10 control embryos and 14 *air-2(or207ts)* embryos used to generate the curves in A and B were the same as those used to calculate the rates in Fig. 4 D. (C) For embryos analyzed in parallel in the single experiment shown in A and B ($n$ = 10–19 embryos per condition), the percentages of embryos that completed cytokinesis are shown. (D) Individual traces of furrow diameter versus time after furrow initiation for individual control and *cyk-1(RNAi) partial* embryos. (E and F) Traces of furrow diameter versus time for individual *zen-4(or153ts)* and *zen-4(or153ts) & cyk-1(RNAi) partial* embryos (E) or *air-2(or207ts)* and *air-2(or207ts) & cyk-1(RNAi) partial* embryos (F). For comparison, mean contractile ring diameter is plotted versus time for control and *cyk-1(RNAi)* embryos. The controls for E and F are the same as those shown in Fig. 3. All imaging was performed using the postmeiotic upshift conditions outlined in Fig. 2 A. Furrow diameters were measured in end-on projections of 11-plane z series collected every 20 s. Traces in A, B, E, and F were smoothed by applying a three-point rolling mean. The circles mark the final diameter before regression. The stars at the end of the trace indicate successful completion of cytokinesis. The arrows to the right of the graphs mark the mean maximum ingression for the indicated conditions. The asterisks indicate a significant difference (two-tailed $t$ test, $P < 0.05$).

the *air-2(or207ts)* phenotype. To test this, we examined the consequences of partially inhibiting *cyk-1*, the gene encoding the cytokinesis formin, under conditions that slow but do not prevent ring constriction (Fig. 5 D) in the two mutant backgrounds. Partial *cyk-1* inhibition strongly enhanced the constriction defect in both the *air-2(or207ts)* and *zen-4(or153ts)* mutants (Fig. 5, E and F), consistent with a similar prior analysis combining a partial loss-of-function *cyk-1* allele with the *air-2(or207ts)* and *zen-4(or153ts)* mutations (Severson et al., 2000). We conclude that the suppression of the *air-2(or207ts)* constriction defect is specific to anillin and the septins. The differential suppression of the *air-2(or207ts)* constriction defect by inhibition of septins or partial inhibition of anillin provides additional genetic evidence for the idea that centralspindlin and the CPC promote contractile ring constriction via distinct pathways.

### Centralspindlin and the CPC are required for the formation of a compact contractile ring but not for the initial recruitment of contractile ring proteins to the equatorial cortex

Shortly after anaphase onset, contractile ring components including anillin and myosin II accumulate on the cortex at the cell equator to form a broad equatorial band (Fig. 6 A, boxed area), and the cortex is deformed to give the initially oval embryo a peanut shape. This deformation is followed by furrow involution, during which the back-to-back plasma membranes of the nascent blastomeres become juxtaposed to one another, and the accumulation of contractile proteins is limited to a compact contractile ring at the furrow tip (Fig. 7, A and B; and Fig. S3). To pinpoint the step that requires centralspindlin and the CPC, we used quantitative methods to monitor the two steps: formation of the equatorial band and assembly of the compact mature contractile ring. We used a cortical imaging method (Lewellyn et al., 2010) to monitor the accumulation of GFP:anillin$^{ANI-1}$ and NMY-2:GFP in the equatorial band. In control embryos, GFP:anillin$^{ANI-1}$ and NMY-2:GFP accumulated on the equatorial cortex during an 80–100-s interval immediately after anaphase onset (Fig. 6, C–F; Lewellyn et al., 2010), forming a band that peaks at ∼60% of embryo length. Furrow involution occurs ∼10 s after the equatorial band reaches its maximum intensity (Lewellyn et al., 2010). Similar accumulation of both markers was observed in control and Aurora B$^{AIR-2}$– and MKLP1$^{ZEN-4}$-depleted embryos (Fig. 6, B–F; and Videos 8 and 9), indicating that neither centralspindlin nor the CPC is essential for the initial enrichment of contractile ring proteins on the equatorial cortex.

After furrow involution, we used a central plane imaging method to measure the amount of NMY-2:GFP in the contractile ring at the furrow tip. Mean intensity linescans along the furrow when the ring had closed to 50% of its initial diameter (Fig. 7 C) revealed a bright compact signal in control embryos (Fig. 7, D and E, black) that was dramatically diminished in upshifted *air-2(or207ts)* and *zen-4(or153ts)* embryos (Fig. 7, D and E, blue and red). We conclude that centralspindlin and the CPC are specifically required to assemble a compact mature contractile ring and that this is a genetically distinct step from the initial accumulation of contractile ring proteins in an equatorial band. Septin$^{UNC-59}$ depletion led to a moderate increase in the amount of NMY-2:GFP in the contractile ring in otherwise normal embryos (Fig. 7, D and E, gray). Consistent with the partial rescue of ingression, septin depletion restored the amount of NMY-2:GFP at the furrow tip to a normal level in *air-2(or207ts)* mutant embryos (Fig. 7, D and E, orange) but did not alter the extent of NMY-2:GFP accumulation in the *zen-4(or153ts)* background (Fig. 7, D and E, green). We conclude that septin inhibition differentially restores contractile ring assembly in the *air-2(or207ts)* but not the *zen-4(or153ts)* mutant.

## Discussion

The results in the previous section indicate that the CPC kinase Aurora B$^{AIR-2}$ and the centralspindlin component MKLP1$^{ZEN-4}$ make independent contributions to ring assembly and constriction. In support of this conclusion, distinct perturbations alleviate the constriction defects in Aurora B$^{AIR-2}$–inhibited versus MKLP1$^{ZEN-4}$-inhibited embryos. Furthermore, we pinpoint the step at which centralspindlin and CPC act to control constriction, which is the transition from a broad equatorial band to a compact mature contractile ring. Cumulatively, these findings argue against the idea that a linear pathway involving the CPC and centralspindlin governs the assembly and constriction of the contractile ring.

### Contractile ring assembly occurs in two genetically separable steps

A key finding of our work is that contractile ring assembly occurs in two genetically separable steps. In the first step, which we term "equatorial band formation," contractile ring proteins accumulate on the embryo cortex in a broad band that encircles the cell equator (Fig. 6 A). The second step transforms the sheet-like equatorial band into a ribbon-like contractile ring that sits at the furrow tip. During this second step, the equatorial band folds in half to form a furrow that extends into the embryo interior. Contractile ring proteins become enriched in a ribbon along the furrow tip (the contractile ring) and are depleted from the region behind the tip (Fig. 7, A and B).

Our data indicate that centralspindlin and the CPC are not required for equatorial band assembly (Lewellyn et al., 2010; and this study); instead, both function in the equatorial band to contractile ring transition. Equatorial band formation requires RhoA activation and proper centrosomal aster separation (Lewellyn et al., 2010). A working model for equatorial band formation is that RhoA is globally up-regulated upon entry into anaphase (Canman et al., 2000; Foe et al., 2000; Shuster and Burgess, 2002; Straight et al., 2003; Foe and von Dassow, 2008), and this global activation is patterned by the centrosomal asters, which inhibit cortical contractility at the cell poles to generate the equatorial band (Wolpert, 1960; White and Borisy, 1983; Werner et al., 2007; Chen et al., 2008; Foe and von Dassow, 2008; Zhou and Wang, 2008). Our results suggest that in *C. elegans*, centralspindlin and the CPC do not contribute to the initial global RhoA activation or its refinement to form the equatorial band.

### Centralspindlin and the CPC make independent contributions that control conversion of the equatorial band into a contractile ring

Previous work placed the CPC and centralspindlin in a linear pathway that governs midzone assembly (Severson et al., 2000). The CPC promotes centralspindlin targeting to the midzone by phosphorylating MKLP1 (Kaitna et al., 2000; Severson et al., 2000; Giet and Glover, 2001; Hauf et al., 2003; Verbrugghe and White, 2004; Guse et al., 2005; Zhu et al., 2005; Douglas et al., 2010). Centralspindlin, in turn, has been proposed to control Rho activation at the cell equator by tethering the RhoGEF Ect2 to the midzone in a polo-kinase–dependent fashion (Yüce et al., 2005; Zhao and Fang, 2005; Chalamalasetty et al., 2006; Kamijo et al., 2006; Nishimura and Yonemura, 2006; Brennan et al., 2007; Burkard et al., 2007; Petronczki et al., 2007). This mechanism predicts that the linear relationship between the CPC and

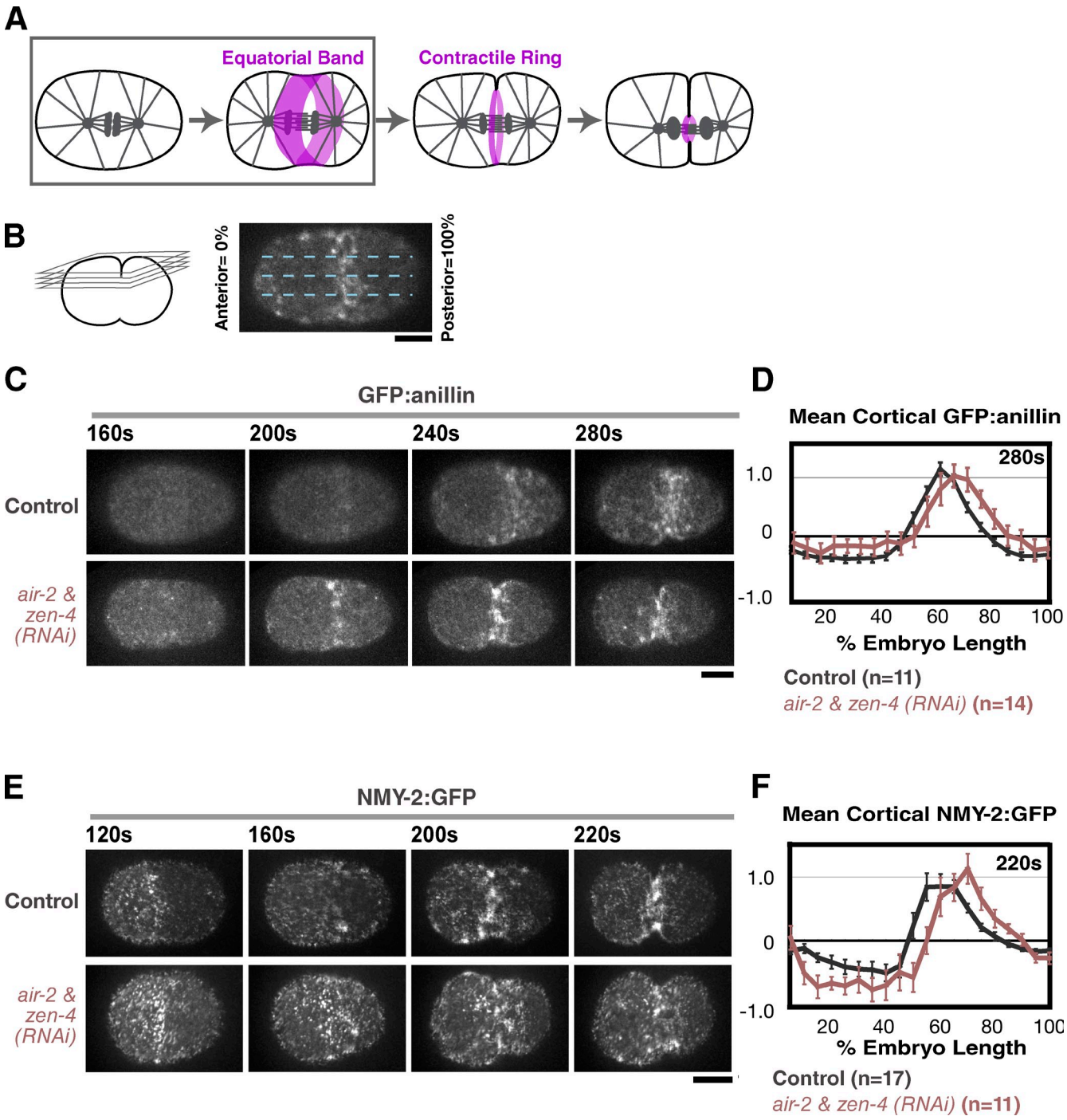


Figure 6. **Simultaneous inhibition of centralspindlin and the CPC does not affect the initial recruitment of contractile ring proteins to the equatorial cortex.** (A) The schematic highlights the first step in cytokinesis (boxed area), formation of the equatorial band. (B) A schematic of the method used to analyze formation of the equatorial band in D and F (Lewellyn et al., 2010). Spinning disk confocal optics were used to collect a 4 × 1–µm z series containing the embryo cortex every 20 s, and a maximum intensity projection was generated for each time point. A 50-pixel-wide line (approximately half the embryo width) was drawn across the projection, and embryos were divided into 20 equal length segments from anterior (0%) to posterior (100%). The mean GFP:anillin$^{ANI\text{-}1}$ or NMY-2:GFP in each segment, after subtraction of a background measurement for that segment made just before anaphase onset (120–160 s after NEBD; before detectable accumulation at the equator), was calculated for each time point. (C and E) Maximum intensity projections of the cortex in control and *zen-4 & air-2(RNAi)* embryos expressing GFP:anillin$^{ANI\text{-}1}$ (C) or NMY-2:GFP (E). (D and F) The mean postanaphase accumulation of cortical GFP:anillin$^{ANI\text{-}1}$ and NMY-2:GFP was quantified as a function of embryo length at the indicated time points after NEBD. The values for each dataset were normalized by dividing all intensity values by the mean value for controls (55–65% embryo length) imaged in parallel at the time point when band formation was maximal. Error bars are SEM. Bars, 10 µm.

centralspindlin during midzone assembly should translate into a linear relationship during the regulation of contractile ring assembly. In particular, two predictions of this model are that targeting of centralspindlin to the midzone is critical for its role in cytokinesis and that a key function of the CPC in contractile ring assembly is to localize/activate centralspindlin.

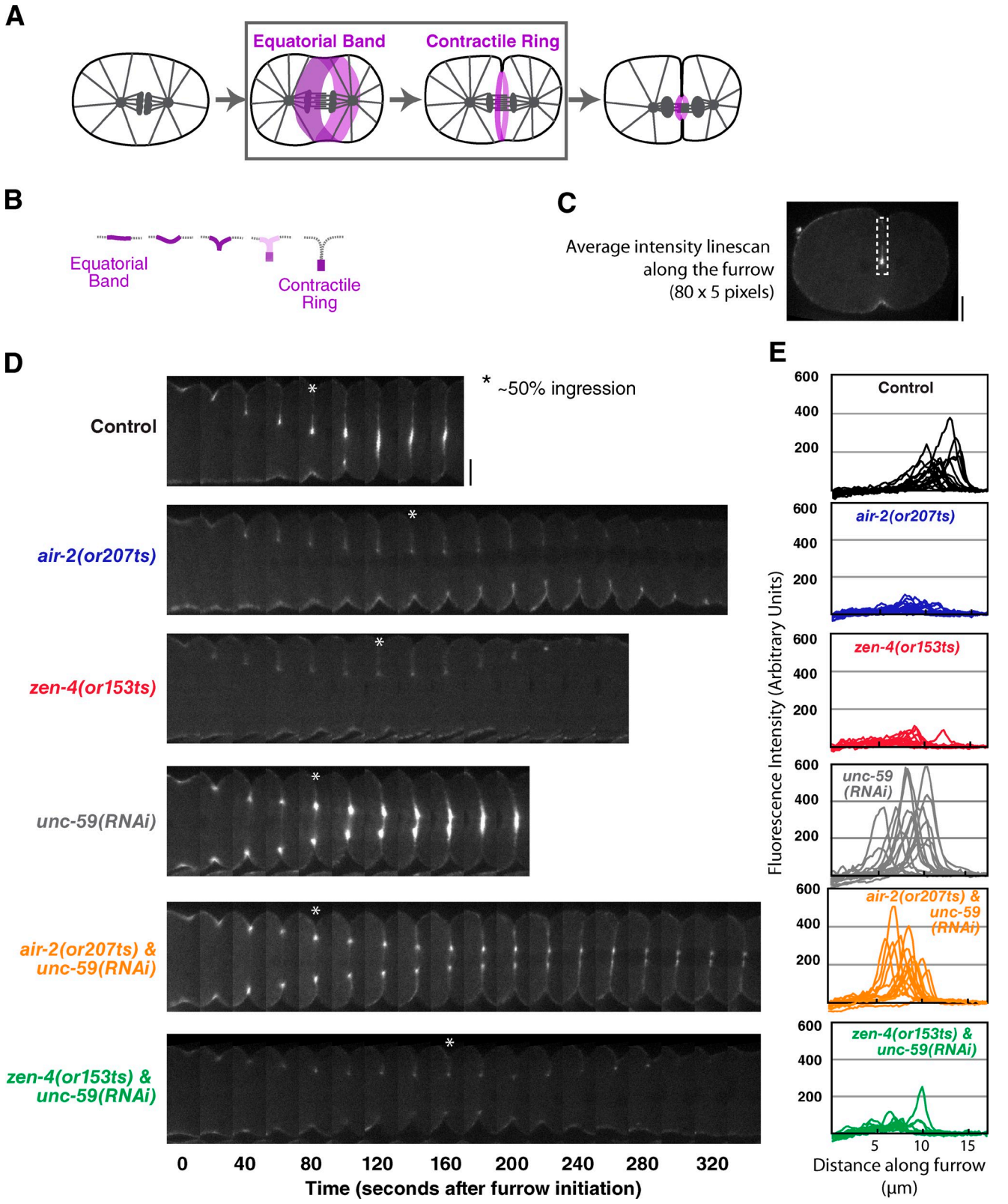


Figure 7. **Inhibition of septin$^{UNC-59}$ rescues the contractile ring assembly defect in Aurora B$^{AIR-2}$– but not MKLP1$^{ZEN-4}$-inhibited embryos.** (A and B) The schematics highlight the second step in cytokinesis (A, boxed area), assembly of the contractile ring. During this step, the cortex folds in, and contractile ring proteins become concentrated in a compact ring that sits at the furrow tip and are cleared from the remainder of the equatorial cortex (illustrated in B; also see Fig. S3). (C) A schematic of the method used to analyze myosin accumulation at the furrow tip. At the time point when the furrow had closed to ~50% of its initial diameter, a mean linescan (80 pixels long and 5 pixels wide) was drawn from the edge of the embryo along the furrow toward the tip. (D) Representative montages of the furrow region for each condition are shown. The asterisks mark the time point when the furrow had closed to ~50% of its initial diameter. (E) The individual linescans for all embryos (after subtraction of cytoplasmic background) are plotted versus distance along the furrow. All imaging was performed using the postmeiotic upshift conditions outlined in Fig. 2 A. Bars, 10 µm.

If the key role of the CPC in contractile ring assembly is to target centralspindlin, simultaneous inhibition of the CPC and centralspindlin is expected to result in the same phenotype seen when either complex is inhibited alone. Instead, we observed an additive effect on constriction rate when we simultaneously inhibited both complexes. The fact that inhibition of the CPC in a centralspindlin-null background leads to an additive reduction in the constriction rate argues that targeting/activating centralspindlin is not the primary contribution that the CPC makes to contractile ring assembly.

Similarly, because centralspindlin is delocalized by CPC inhibition, the fact that centralspindlin inhibition in a CPC-null background leads to an additive reduction in constriction rate suggests that the localization of centralspindlin to the midzone is not critical for its main role in contractile ring assembly. This result is consistent with the finding that the midzone targeting of centralspindlin is dramatically reduced when $PRC1^{SPD-1}$ is inhibited in *C. elegans* or human cells, yet furrowing is not significantly affected (Verbrugghe and White, 2004; Mollinari et al., 2005), and with previous work suggesting that centralspindlin targets to the cortex and its cortical, rather than midzone, localization is key to cytokinesis success (D'Avino et al., 2006; Nishimura and Yonemura, 2006; Verbrugghe and White, 2007). It is worth noting that in both *Drosophila* and *C. elegans*, the homologues of the Ect2 guanine nucleotide exchange factor localize to the cortex but have not been detected at the midzone (Prokopenko et al., 1999, Motegi and Sugimoto, 2006; and unpublished data), making it unclear whether the role of centralspindlin in targeting Ect2 to the midzone is conserved. Instead, the critical conserved function of centralspindlin in constriction seems to depend on its GAP activity toward Rho family GTPases. In *C. elegans*, mutations in $MgcRacGAP^{CYK-4}$ predicted to disrupt its GAP activity, but which do not alter midzone assembly, exhibit a constriction defect identical to depletion or loss-of-function mutants of centralspindlin (Canman et al., 2008). The GAP activity of MgcRacGAP has also been shown to be essential for cytokinesis in *Drosophila* and *Xenopus* (Zavortink et al., 2005; Miller and Bement, 2009). Cumulatively, these studies challenge the current dominant model, suggesting that the GAP activity of MgcRacGAP and its ability to target to the cortex, rather than its ability to target to the midzone and recruit the Ect2 guanine nucleotide exchange factor, mediate its conserved function in contractile ring assembly.

### A link between the septins and CPC function during cytokinesis

Our analysis revealed an unexpected specific genetic interaction between the septins and the CPC: depletion of the septins or partial depletion of anillin restored contractile ring assembly and allowed cytokinesis completion in Aurora $B^{AIR-2}$–inhibited embryos. This observation is significant because, to our knowledge, this is the first time septin or anillin inhibition has been found to alleviate, rather than aggravate, a constriction phenotype. The septins are conserved GTP-binding proteins that form hetero-oligomers that polymerize to form a membrane-associated filament lattice (Rodal et al., 2005; Vrabioiu and Mitchison, 2006; Barral and Kinoshita, 2008; Weirich et al., 2008). Septin depletion leads to low-level cytokinesis failure and enhances the constriction defect resulting from inhibiting myosin activation by depletion of Rho $kinase^{LET-502}$, suggesting that it makes the contractile ring mechanically less robust (Maddox et al., 2007). Consistent with this idea, septin inhibition mildly enhances the *zen-4(or153ts)* constriction defect (Fig. 5 A). These observations indicate that the significant rescue of contractile ring assembly and cytokinesis completion in the *air-2(or207ts)* background reflects a specific and potentially mechanistically revealing genetic interaction.

The restoration of contractile ring assembly in Aurora $B^{AIR-2}$–inhibited embryos after codepletion of the septins raises the possibility that the CPC facilitates contractile ring assembly by promoting septin reorganization. Work in budding yeast provides precedent for a dramatic reorganization of the septins immediately before ring constriction. Fluorescence polarization microscopy and analysis by FRAP has shown that septin filaments at the division site are initially frozen and oriented parallel to the mother–daughter axis but then become dynamic and undergo a 90° rotation immediately before contractile ring constriction (Caviston et al., 2003; Dobbelaere et al., 2003; Vrabioiu and Mitchison, 2006). Budding yeast septin dynamics are controlled by phosphorylation (Versele and Thorner, 2005). It is thus tempting to speculate that in animal cells, the CPC promotes septin reorganization during contractile ring assembly, and this reorganization is important for the transition from the equatorial band to the contractile ring. Analysis by mass spectrometry of immunoprecipitations (IPs) of the two septins (UNC-59 and UNC-61) and three of the four CPC subunits (ICP-1, AIR-2, and CSC-1) from *C. elegans* embryo extracts revealed the presence of the septins at low coverage in one out of two $INCENP^{ICP-1}$ IPs and one out of two Aurora $B^{AIR-2}$ IPs. However, the septins were also observed at a similar level of coverage in IPs of SPD-1, ZEN-4, NMY-2, and cofilin, and CPC subunits were not detected in the septin IPs (unpublished data), making it unclear as to whether the presence of the septins in the ICP-1 and AIR-2 IPs reflects a specific interaction. A detailed mechanistic investigation of the relationship between the CPC and the septins will require future efforts.

In summary, we show that although the CPC and centralspindlin act in a linear pathway during midzone assembly, they make independent contributions to contractile ring assembly, controlling the structural transition from broadly enriched contractile proteins at the cell equator to a compact contractile ring at the furrow tip. Septin inhibition specifically alleviates the ring assembly and constriction defect observed in CPC-inhibited embryos. These findings have important implications for how the widely conserved centralspindlin and CPC provide their essential contributions during cytokinesis.

## Materials and methods

#### Strains and live imaging

The genotypes of all strains used are listed in Table S1. Strains were maintained at 20°C, except for temperature-sensitive strains, which were maintained at 16°C. Strains used in each experiment were as follows: Fig. 1 (OD95, OD105, OD106, and OD488); Fig. 2 C (OD52 and OD253); Fig. 2 D (EU630); Fig. 3 (A–C), Figs. 4 and 5, and Fig. S2 (OD95, OD105,

and OD106); Fig. 3 D (OD27); Fig. 6 (OD38 and JJ1473); and Fig. 7 (JJ1473, OD236, and OD283). For the premeiotic shifting experiments in Fig. 1, worms were put into a room preheated to the restrictive temperature (~26.5°C) 30–60 min before dissection. For postmeiotic upshift experiments, temperature-sensitive strains were maintained at the permissive temperature (~16°C) until dissection by placing inverted plates over bubble wrap on top of ice in an ice bucket. Dissections were performed in a room preheated to the restrictive temperature. The temperature was monitored using a thermometer (Digi-Sense Type T Thermocouple; Cole-Parmer).

Live imaging was performed on newly fertilized embryos mounted and obtained by dissecting gravid hermaphrodites in M9 medium (Brenner, 1974), collecting the embryos with a mouth pipette, placing them on a 2% agarose pad, and covering them with an 18 × 18–mm coverslip. Embryos were filmed using a spinning disk confocal system (Andor Revolution XD Confocal System; Andor Technology) with a confocal scanner unit (CSU-10; Yokogawa) mounted on an inverted microscope (TE2000-E; Nikon) equipped with a 60× 1.4 NA PlanApochromat lens and solid-state 100-mW lasers. An electron multiplication back-thinned charge-coupled device camera (iXon; Andor Technology) with no binning was used for the experiment in Fig. 2 C. For all other experiments, a high-resolution interline charge-coupled device camera (Clara; Andor Technology) was used with 2 × 2 binning. For end-on projections, 11 z sections were collected at 2.5-µm intervals, and the region of the furrow was isolated, projected, and rotated by 90° using MetaMorph software (Molecular Devices). For cortical imaging, four z sections were collected at 1-µm intervals. For the myosin furrow intensity measurements in Fig. 7, six z sections were collected at 2-µm intervals every 20 s. At each time point, the plane in which the furrow was in focus was chosen, and a montage of the furrow region over time was constructed. A mean intensity linescan (80 pixels long and 5 pixels wide) was drawn from the edge of the embryo along the furrow. The linescan extended past the furrow tip and into the embryo cytoplasm. The intensity along the furrow was calculated by subtracting the cytoplasmic background (mean of the final five values of the linescan) from each value. The results were plotted versus position along the furrow. Images were cropped and scaled in Photoshop (Adobe), and figures were constructed in Illustrator (Adobe).

### Immunofluorescence

Immunofluorescence was performed by cutting six worms in half with a scalpel in a 2.2-µl drop of water on a slide pretreated by coating the center with a thin layer of 1 mg/ml poly-lysine (P-1524; Sigma-Aldrich) dissolved in PBS (BP665-1; Thermo Fisher Scientific), drying the layer down briefly on a hot plate, and then baking in a 100°C oven for 30 min immediately before use. The drop was covered with a 10-mm square coverslip, and the slide was immediately plunged into liquid nitrogen. The slides were removed from the liquid nitrogen, the coverslip was popped off, and the slides were placed into –20°C methanol for 20 min followed by rehydration in PBS (twice for 5 min) at room temperature. Slides were removed from the PBS and dried with Kimwipes (Kimberly-Clark), avoiding the area with the adhered embryos, which was circled with a PAP pen. Embryos were blocked by pipeting on 50 µl AbDil and incubating for 20 min and then were incubated at 4°C with FITC-labeled α-tubulin antibodies (1:500 DM1-α; Abcam) and 1 µg/ml each of antibodies to ZEN-4 and AIR-2 (directly labeled with Cy3 or Cy5; Lewellyn et al., 2010) diluted in Abdil. Embryos were washed three times with PBST (PBS + 0.1% Triton X-100) and once with PBST + 1 µg/ml Hoechst and mounted in 4 µl of 0.5% *p*-phenylenediamine, 20 mM Tris-Cl, pH 8.8, and 90% glycerol under an 18 × 18–mm coverslip. Images were acquired using a 100× 1.35 NA U-Planapo oil objective lens (Olympus) mounted on a DeltaVision system (Applied Precision) that included a microscope (IX70; Olympus) equipped with a camera (CoolSnap CCD; Roper Scientific). All fixed images are of three-dimensional widefield datasets that were computationally deconvolved and projected using Softworx software (Applied Precision). Images were cropped and scaled, and color overlays were generated in Photoshop. Figures were constructed in Illustrator.

### RNA-mediated interference

Double-stranded RNAs (dsRNAs) were prepared by using the oligonucleotides listed in Table S2 to amplify regions from N2 genomic or specific cDNAs (provided by Y. Kohara, National Institute of Genetics, Mishima, Japan). PCR reactions were cleaned (QIAGEN) and used as templates for 25 µl T3 and T7 transcription reactions (Invitrogen), which were combined and cleaned using the RNeasy kit (QIAGEN). RNA eluted with 50 µl $H_2O$ was mixed with 25 µl of 3× injection buffer (IX = 20 mM $KPO_4$, pH 7.5, 3 mM K-Citrate, pH 7.5, and 2% PEG 6000) and annealed by incubating at 68°C for 10 min followed by 37°C for 30 min. L4 hermaphrodites were injected with dsRNA and incubated at 20°C (or 16°C for the mutant strains) for 45–48 h. For double depletions, RNAs were mixed to obtain equal concentrations for each RNA. For the partial *cyk-1(RNAi)* in Fig. 5, young adult worms were injected with dsRNA and incubated at 16°C for 24 h before imaging.

### Western blotting

Western blotting was performed by transferring ~80 control, *air-2(RNAi)*, *zen-4(RNAi)*, or *air-2 & zen-4(RNAi)* worms into an Eppendorf containing 1 ml of M9 with 0.1% Triton X-100 and pelleting them by centrifuging at 200 *g* for 1 min. Worms were washed and pelleted three times in 1 ml of M9 + 0.1% Triton X-100. After the last wash, excess buffer was removed, leaving 60 µl. 20 µl of 4× sample buffer was added, and the samples were placed in a sonicating water bath at ~70°C for 10 min and then at 95°C for 5 min in a heating block before freezing. Samples were thawed, heated to 95°C for 5 min, and loaded on an SDS-PAGE gel. Western blots were initially probed using 2 µg/ml of rabbit anti–ZEN-4 or anti–AIR-2, which was detected using an HRP-conjugated secondary antibody (1:10,000; Bio-Rad Laboratories). The same blot was subsequently probed for α-tubulin using the monoclonal DM1α (1:100; Sigma-Aldrich) followed by an alkaline-phosphatase–conjugated anti–mouse secondary antibody (1:3,750; Jackson ImmunoResearch Laboratories, Inc.). Serial dilutions of a control lysate made from uninjected N2 worms were used to quantify the amount of Aurora $B^{AIR\text{-}2}$ or $MKLP1^{ZEN\text{-}4}$ in the RNAi samples. The Western blot was analyzed by drawing a box around each band and measuring the signal above background. Signals from the serial dilution of the control lysate were used to generate a standard curve that was used to calculate the amount in the RNAi lanes.

### Online supplemental material

Tables S1 and S2 list the strains and dsRNAs used in this study, respectively. Fig. S1 shows a Western blot of control, *air-2(RNAi)*, *zen-4(RNAi)*, and *air-2 & zen-4(RNAi)* worms. Fig. S2 shows that the contractile ring constriction defect in Aurora $B^{AIR\text{-}2}$–inhibited embryos is alleviated by partial depletion of $anillin^{ANI\text{-}1}$. Fig. S3 shows the two steps in contractile ring assembly. Video 1, which corresponds to Fig. 1 A, shows that simultaneous depletion of Aurora $B^{AIR\text{-}2}$ and $MKLP1^{ZEN\text{-}4}$ leads to an additive contractile ring constriction defect. Video 2, which corresponds to Fig. 1 C, shows that codepletion of Aurora $B^{AIR\text{-}2}$ and $MKLP1^{ZEN\text{-}4}$ in the upshifted double mutant results in an additive contractile ring constriction defect versus depletion of Aurora $B^{AIR\text{-}2}$ or $MKLP1^{ZEN\text{-}4}$ alone in the corresponding upshifted single mutants. Video 3, which corresponds to Fig. 2 C, shows that a temperature-sensitive Aurora $B^{AIR\text{-}2}$ mutant can be used to bypass the meiotic defects resulting from CPC inhibition. Video 4, which corresponds to Fig. 3 D, shows that Aurora $B^{AIR\text{-}2}$ localizes to microtubules emanating from the chromosomes into the region between the separating chromosomes in *C. elegans* embryos depleted of $PRC1^{SPD\text{-}1}$ or $MKLP1^{ZEN\text{-}4}$. Video 5, which corresponds to the control sequences in Fig. 5 (A and B) and Fig. S2 (A and B), shows that cytokinesis completes successfully in *C. elegans* embryos depleted of $septin^{UNC\text{-}59}$ or $anillin^{ANI\text{-}1}$. Video 6, which corresponds to Fig. 5 B and Fig. S2 B, shows that depletion of $septin^{UNC\text{-}59}$ or partial depletion of $anillin^{ANI\text{-}1}$ alleviates the constriction defect in Aurora $B^{AIR\text{-}2}$–inhibited *C. elegans* embryos. Video 7, which corresponds to Fig. 5 A and Fig. S2 A, shows that depletion of $septin^{UNC\text{-}59}$ or partial depletion of $anillin^{ANI\text{-}1}$ does not alleviate the constriction defect in *C. elegans zen-4(or153ts)* embryos. Video 8, which corresponds to Fig. 6 C, shows that codepletion of centralspindlin and the CPC does not affect recruitment of GFP:$anillin^{ANI\text{-}1}$ to the equatorial band. Video 9, which corresponds to Fig. 6 E, shows that codepletion of centralspindlin and the CPC does not affect recruitment of NMY-2:GFP to an equatorial band. Online supplemental material is available at http://www.jcb.org/cgi/content/full/jcb.201008138/DC1.

We thank members of the Oegema and Desai laboratories, especially J. Canman, for their support. Y. Kohara provided gene-specific cDNAs.

K. Oegema and A. Desai receive salary and additional support from the Ludwig Institute for Cancer Research. L. Lewellyn was supported by the University of California, San Diego Genetics Training Program (T32 GM008666) funded by the National Institutes of Health/National Institute of General Medical Sciences.

Submitted: 24 August 2010
Accepted: 3 March 2011

## References


Barral, Y., and M. Kinoshita. 2008. Structural insights shed light onto septin assemblies and function. *Curr. Opin. Cell Biol.* 20:12–18. doi:10.1016/j.ceb.2007.12.001

Brennan, I.M., U. Peters, T.M. Kapoor, and A.F. Straight. 2007. Polo-like kinase controls vertebrate spindle elongation and cytokinesis. *PLoS ONE*. 2:e409. doi:10.1371/journal.pone.0000409

Brenner, S. 1974. The genetics of *Caenorhabditis elegans. Genetics*. 77:71–94.

Burkard, M.E., C.L. Randall, S. Larochelle, C. Zhang, K.M. Shokat, R.P. Fisher, and P.V. Jallepalli. 2007. Chemical genetics reveals the requirement for Polo-like kinase 1 activity in positioning RhoA and triggering cytokinesis in human cells. *Proc. Natl. Acad. Sci. USA*. 104:4383–4388. doi:10.1073/pnas.0701140104

Canman, J.C., D.B. Hoffman, and E.D. Salmon. 2000. The role of pre- and post-anaphase microtubules in the cytokinesis phase of the cell cycle. *Curr. Biol.* 10:611–614. doi:10.1016/S0960-9822(00)00490-5

Canman, J.C., L. Lewellyn, K. Laband, S.J. Smerdon, A. Desai, B. Bowerman, and K. Oegema. 2008. Inhibition of Rac by the GAP activity of centralspindlin is essential for cytokinesis. *Science*. 322:1543–1546. doi:10.1126/science.1163086

Carmena, M. 2008. Cytokinesis: the final stop for the chromosomal passengers. *Biochem. Soc. Trans.* 36:367–370. doi:10.1042/BST0360367

Carmena, M., S. Ruchaud, and W.C. Earnshaw. 2009. Making the Auroras glow: regulation of Aurora A and B kinase function by interacting proteins. *Curr. Opin. Cell Biol.* 21:796–805. doi:10.1016/j.ceb.2009.09.008

Carvalho, A., A. Desai, and K. Oegema. 2009. Structural memory in the contractile ring makes the duration of cytokinesis independent of cell size. *Cell*. 137:926–937. doi:10.1016/j.cell.2009.03.021

Caviston, J.P., M. Longtine, J.R. Pringle, and E. Bi. 2003. The role of Cdc42p GTPase-activating proteins in assembly of the septin ring in yeast. *Mol. Biol. Cell*. 14:4051–4066. doi:10.1091/mbc.E03-04-0247

Cesario, J.M., J.K. Jang, B. Redding, N. Shah, T. Rahman, and K.S. McKim. 2006. Kinesin 6 family member Subito participates in mitotic spindle assembly and interacts with mitotic regulators. *J. Cell Sci.* 119:4770–4780. doi:10.1242/jcs.03235

Chalamalasetty, R.B., S. Hümmer, E.A. Nigg, and H.H. Silljé. 2006. Influence of human Ect2 depletion and overexpression on cleavage furrow formation and abscission. *J. Cell Sci.* 119:3008–3019. doi:10.1242/jcs.03032

Chen, W., M. Foss, K.F. Tseng, and D. Zhang. 2008. Redundant mechanisms recruit actin into the contractile ring in silkworm spermatocytes. *PLoS Biol.* 6:e209. doi:10.1371/journal.pbio.0060209

D'Avino, P.P. 2009. How to scaffold the contractile ring for a safe cytokinesis - lessons from Anillin-related proteins. *J. Cell Sci.* 122:1071–1079. doi:10.1242/jcs.034785

D'Avino, P.P., and D.M. Glover. 2009. Cytokinesis: mind the GAP. *Nat. Cell Biol.* 11:112–114. doi:10.1038/ncb0209-112

D'Avino, P.P., M.S. Savoian, and D.M. Glover. 2004. Mutations in sticky lead to defective organization of the contractile ring during cytokinesis and are enhanced by Rho and suppressed by Rac. *J. Cell Biol.* 166:61–71. doi:10.1083/jcb.200402157

D'Avino, P.P., M.S. Savoian, and D.M. Glover. 2005. Cleavage furrow formation and ingression during animal cytokinesis: a microtubule legacy. *J. Cell Sci.* 118:1549–1558. doi:10.1242/jcs.02335

D'Avino, P.P., M.S. Savoian, L. Capalbo, and D.M. Glover. 2006. RacGAP50C is sufficient to signal cleavage furrow formation during cytokinesis. *J. Cell Sci.* 119:4402–4408. doi:10.1242/jcs.03210

Dobbelaere, J., M.S. Gentry, R.L. Hallberg, and Y. Barral. 2003. Phosphorylation-dependent regulation of septin dynamics during the cell cycle. *Dev. Cell*. 4:345–357. doi:10.1016/S1534-5807(03)00061-3

Douglas, M.E., T. Davies, N. Joseph, and M. Mishima. 2010. Aurora B and 14-3-3 coordinately regulate clustering of centralspindlin during cytokinesis. *Curr. Biol.* 20:927–933. doi:10.1016/j.cub.2010.03.055

Eggert, U.S., T.J. Mitchison, and C.M. Field. 2006. Animal cytokinesis: from parts list to mechanisms. *Annu. Rev. Biochem.* 75:543–566. doi:10.1146/annurev.biochem.74.082803.133425

Foe, V.E., and G. von Dassow. 2008. Stable and dynamic microtubules coordinately shape the myosin activation zone during cytokinetic furrow formation. *J. Cell Biol.* 183:457–470. doi:10.1083/jcb.200807128

Foe, V.E., C.M. Field, and G.M. Odell. 2000. Microtubules and mitotic cycle phase modulate spatiotemporal distributions of F-actin and myosin II in *Drosophila* syncytial blastoderm embryos. *Development*. 127:1767–1787.

Gassmann, R., A. Carvalho, A.J. Henzing, S. Ruchaud, D.F. Hudson, R. Honda, E.A. Nigg, D.L. Gerloff, and W.C. Earnshaw. 2004. Borealin: a novel chromosomal passenger required for stability of the bipolar mitotic spindle. *J. Cell Biol.* 166:179–191. doi:10.1083/jcb.200404001

Giet, R., and D.M. Glover. 2001. *Drosophila* aurora B kinase is required for histone H3 phosphorylation and condensin recruitment during chromosome condensation and to organize the central spindle during cytokinesis. *J. Cell Biol.* 152:669–682. doi:10.1083/jcb.152.4.669

Glotzer, M. 2005. The molecular requirements for cytokinesis. *Science*. 307:1735–1739. doi:10.1126/science.1096896

Glotzer, M. 2009. Cytokinesis: GAP gap. *Curr. Biol.* 19:R162–R165. doi:10.1016/j.cub.2008.12.028

Guse, A., M. Mishima, and M. Glotzer. 2005. Phosphorylation of ZEN-4/MKLP1 by aurora B regulates completion of cytokinesis. *Curr. Biol.* 15:778–786. doi:10.1016/j.cub.2005.03.041

Hauf, S., R.W. Cole, S. LaTerra, C. Zimmer, G. Schnapp, R. Walter, A. Heckel, J. van Meel, C.L. Rieder, and J.M. Peters. 2003. The small molecule Hesperadin reveals a role for Aurora B in correcting kinetochore-microtubule attachment and in maintaining the spindle assembly checkpoint. *J. Cell Biol.* 161:281–294. doi:10.1083/jcb.200208092

Jantsch-Plunger, V., P. Gönczy, A. Romano, H. Schnabel, D. Hamill, R. Schnabel, A.A. Hyman, and M. Glotzer. 2000. CYK-4: A Rho family gtpase activating protein (GAP) required for central spindle formation and cytokinesis. *J. Cell Biol.* 149:1391–1404. doi:10.1083/jcb.149.7.1391

Kaitna, S., M. Mendoza, V. Jantsch-Plunger, and M. Glotzer. 2000. Incenp and an aurora-like kinase form a complex essential for chromosome segregation and efficient completion of cytokinesis. *Curr. Biol.* 10:1172–1181. doi:10.1016/S0960-9822(00)00721-1

Kamijo, K., N. Ohara, M. Abe, T. Uchimura, H. Hosoya, J.S. Lee, and T. Miki. 2006. Dissecting the role of Rho-mediated signaling in contractile ring formation. *Mol. Biol. Cell*. 17:43–55. doi:10.1091/mbc.E05-06-0569

Kurasawa, Y., W.C. Earnshaw, Y. Mochizuki, N. Dohmae, and K. Todokoro. 2004. Essential roles of KIF4 and its binding partner PRC1 in organized central spindle midzone formation. *EMBO J.* 23:3237–3248. doi:10.1038/sj.emboj.7600347

Lewellyn, L., J. Dumont, A. Desai, and K. Oegema. 2010. Analyzing the effects of delaying aster separation on furrow formation during cytokinesis in the *Caenorhabditis elegans* embryo. *Mol. Biol. Cell*. 21:50–62. doi:10.1091/mbc.E09-01-0089

Maddox, A.S., L. Lewellyn, A. Desai, and K. Oegema. 2007. Anillin and the septins promote asymmetric ingression of the cytokinetic furrow. *Dev. Cell*. 12:827–835. doi:10.1016/j.devcel.2007.02.018

Matsumura, F. 2005. Regulation of myosin II during cytokinesis in higher eukaryotes. *Trends Cell Biol.* 15:371–377. doi:10.1016/j.tcb.2005.05.004

Miller, A.L., and W.M. Bement. 2009. Regulation of cytokinesis by Rho GTPase flux. *Nat. Cell Biol.* 11:71–77. doi:10.1038/ncb1814

Minoshima, Y., T. Kawashima, K. Hirose, Y. Tonozuka, A. Kawajiri, Y.C. Bao, X. Deng, M. Tatsuka, S. Narumiya, W.S. May Jr., et al. 2003. Phosphorylation by aurora B converts MgcRacGAP to a RhoGAP during cytokinesis. *Dev. Cell*. 4:549–560. doi:10.1016/S1534-5807(03)00089-3

Mollinari, C., J.P. Kleman, Y. Saoudi, S.A. Jablonski, J. Perard, T.J. Yen, and R.L. Margolis. 2005. Ablation of PRC1 by small interfering RNA demonstrates that cytokinetic abscission requires a central spindle bundle in mammalian cells, whereas completion of furrowing does not. *Mol. Biol. Cell*. 16:1043–1055. doi:10.1091/mbc.E04-04-0346

Motegi, F., and A. Sugimoto. 2006. Sequential functioning of the ECT-2 RhoGEF, RHO-1 and CDC-42 establishes cell polarity in *Caenorhabditis elegans* embryos. *Nat. Cell Biol.* 8:978–985. doi:10.1038/ncb1459

Murata-Hori, M., K. Fumoto, Y. Fukuta, T. Iwasaki, A. Kikuchi, M. Tatsuka, and H. Hosoya. 2000. Myosin II regulatory light chain as a novel substrate for AIM-1, an aurora/Ipl1p-related kinase from rat. *J. Biochem.* 128:903–907.

Nishimura, Y., and S. Yonemura. 2006. Centralspindlin regulates ECT2 and RhoA accumulation at the equatorial cortex during cytokinesis. *J. Cell Sci.* 119:104–114. doi:10.1242/jcs.02737

Ozlü, N., F. Monigatti, B.Y. Renard, C.M. Field, H. Steen, T.J. Mitchison, and J.J. Steen. 2010. Binding partner switching on microtubules and aurora-B in the mitosis to cytokinesis transition. *Mol. Cell. Proteomics*. 9:336–350. doi:10.1074/mcp.M900308-MCP200

Pavicic-Kaltenbrunner, V., M. Mishima, and M. Glotzer. 2007. Cooperative assembly of CYK-4/MgcRacGAP and ZEN-4/MKLP1 to form the centralspindlin complex. *Mol. Biol. Cell*. 18:4992–5003. doi:10.1091/mbc.E07-05-0468

Petronczki, M., M. Glotzer, N. Kraut, and J.M. Peters. 2007. Polo-like kinase 1 triggers the initiation of cytokinesis in human cells by promoting recruitment of the RhoGEF Ect2 to the central spindle. *Dev. Cell*. 12:713–725. doi:10.1016/j.devcel.2007.03.013

Piekny, A.J., and P.E. Mains. 2002. Rho-binding kinase (LET-502) and myosin phosphatase (MEL-11) regulate cytokinesis in the early *Caenorhabditis elegans* embryo. *J. Cell Sci.* 115:2271–2282.

Powers, J., O. Bossinger, D. Rose, S. Strome, and W. Saxton. 1998. A nematode kinesin required for cleavage furrow advancement. *Curr. Biol.* 8:1133–1136. doi:10.1016/S0960-9822(98)70470-1

Prokopenko, S.N., A. Brumby, L. O'Keefe, L. Prior, Y. He, R. Saint, and H.J. Bellen. 1999. A putative exchange factor for Rho1 GTPase is required for initiation of cytokinesis in *Drosophila. Genes Dev.* 13:2301–2314. doi:10.1101/gad.13.17.2301

Raich, W.B., A.N. Moran, J.H. Rothman, and J. Hardin. 1998. Cytokinesis and midzone microtubule organization in *Caenorhabditis elegans* require the kinesin-like protein ZEN-4. *Mol. Biol. Cell*. 9:2037–2049.

Rodal, A.A., L. Kozubowski, B.L. Goode, D.G. Drubin, and J.H. Hartwig. 2005. Actin and septin ultrastructures at the budding yeast cell cortex. *Mol. Biol. Cell*. 16:372–384. doi:10.1091/mbc.E04-08-0734

Rogers, E., J.D. Bishop, J.A. Waddle, J.M. Schumacher, and R. Lin. 2002. The aurora kinase AIR-2 functions in the release of chromosome cohesion in *Caenorhabditis elegans* meiosis. *J. Cell Biol.* 157:219–229. doi:10.1083/jcb.200110045

Romano, A., A. Guse, I. Krascenicova, H. Schnabel, R. Schnabel, and M. Glotzer. 2003. CSC-1: a subunit of the Aurora B kinase complex that binds to the survivin-like protein BIR-1 and the incenp-like protein ICP-1. *J. Cell Biol.* 161:229–236. doi:10.1083/jcb.200207117

Ruchaud, S., M. Carmena, and W.C. Earnshaw. 2007. Chromosomal passengers: conducting cell division. *Nat. Rev. Mol. Cell Biol.* 8:798–812. doi:10.1038/nrm2257

Schroeder, T.E. 1972. The contractile ring. II. Determining its brief existence, volumetric changes, and vital role in cleaving *Arbacia* eggs. *J. Cell Biol.* 53:419–434. doi:10.1083/jcb.53.2.419

Schroeder, T.E. 1975. Dynamics of the contractile ring. *Soc. Gen. Physiol. Ser.* 30:305–334.

Schumacher, J.M., A. Golden, and P.J. Donovan. 1998. AIR-2: An Aurora/Ipl1-related protein kinase associated with chromosomes and midbody microtubules is required for polar body extrusion and cytokinesis in *Caenorhabditis elegans* embryos. *J. Cell Biol.* 143:1635–1646. doi:10.1083/jcb.143.6.1635

Sellers, J.R., M.D. Pato, and R.S. Adelstein. 1981. Reversible phosphorylation of smooth muscle myosin, heavy meromyosin, and platelet myosin. *J. Biol. Chem.* 256:13137–13142.

Sellers, J.R., J.A. Spudich, and M.P. Sheetz. 1985. Light chain phosphorylation regulates the movement of smooth muscle myosin on actin filaments. *J. Cell Biol.* 101:1897–1902. doi:10.1083/jcb.101.5.1897

Severson, A.F., D.R. Hamill, J.C. Carter, J. Schumacher, and B. Bowerman. 2000. The aurora-related kinase AIR-2 recruits ZEN-4/CeMKLP1 to the mitotic spindle at metaphase and is required for cytokinesis. *Curr. Biol.* 10:1162–1171. doi:10.1016/S0960-9822(00)00715-6

Shuster, C.B., and D.R. Burgess. 2002. Transitions regulating the timing of cytokinesis in embryonic cells. *Curr. Biol.* 12:854–858. doi:10.1016/S0960-9822(02)00838-2

Speliotes, E.K., A. Uren, D. Vaux, and H.R. Horvitz. 2000. The survivin-like *C. elegans* BIR-1 protein acts with the Aurora-like kinase AIR-2 to affect chromosomes and the spindle midzone. *Mol. Cell*. 6:211–223. doi:10.1016/S1097-2765(00)00023-X

Straight, A.F., A. Cheung, J. Limouze, I. Chen, N.J. Westwood, J.R. Sellers, and T.J. Mitchison. 2003. Dissecting temporal and spatial control of cytokinesis with a myosin II Inhibitor. *Science*. 299:1743–1747. doi:10.1126/science.1081412

Verbrugghe, K.J., and J.G. White. 2004. SPD-1 is required for the formation of the spindle midzone but is not essential for the completion of cytokinesis in *C. elegans* embryos. *Curr. Biol.* 14:1755–1760. doi:10.1016/j.cub.2004.09.055

Verbrugghe, K.J., and J.G. White. 2007. Cortical centralspindlin and G alpha have parallel roles in furrow initiation in early *C. elegans* embryos. *J. Cell Sci.* 120:1772–1778. doi:10.1242/jcs.03447

Versele, M., and J. Thorner. 2005. Some assembly required: yeast septins provide the instruction manual. *Trends Cell Biol.* 15:414–424. doi:10.1016/j.tcb.2005.06.007

von Dassow, G. 2009. Concurrent cues for cytokinetic furrow induction in animal cells. *Trends Cell Biol.* 19:165–173. doi:10.1016/j.tcb.2009.01.008

Vrabioiu, A.M., and T.J. Mitchison. 2006. Structural insights into yeast septin organization from polarized fluorescence microscopy. *Nature*. 443:466–469. doi:10.1038/nature05109

Weirich, C.S., J.P. Erzberger, and Y. Barral. 2008. The septin family of GTPases: architecture and dynamics. *Nat. Rev. Mol. Cell Biol.* 9:478–489. doi:10.1038/nrm2407

Werner, M., E. Munro, and M. Glotzer. 2007. Astral signals spatially bias cortical myosin recruitment to break symmetry and promote cytokinesis. *Curr. Biol.* 17:1286–1297. doi:10.1016/j.cub.2007.06.070

White, J.G., and G.G. Borisy. 1983. On the mechanisms of cytokinesis in animal cells. *J. Theor. Biol.* 101:289–316. doi:10.1016/0022-5193(83)90342-9

Wolpert, L. 1960. The mechanics and mechanism of cleavage. *Int. Rev. Cytol.* 10:163–216.

Yoshizaki, H., Y. Ohba, M.C. Parrini, N.G. Dulyaninova, A.R. Bresnick, N. Mochizuki, and M. Matsuda. 2004. Cell type-specific regulation of RhoA activity during cytokinesis. *J. Biol. Chem.* 279:44756–44762. doi:10.1074/jbc.M402292200

Yüce, O., A. Piekny, and M. Glotzer. 2005. An ECT2-centralspindlin complex regulates the localization and function of RhoA. *J. Cell Biol.* 170:571–582. doi:10.1083/jcb.200501097

Zavortink, M., N. Contreras, T. Addy, A. Bejsovec, and R. Saint. 2005. Tum/RacGAP50C provides a critical link between anaphase microtubules and the assembly of the contractile ring in *Drosophila melanogaster. J. Cell Sci.* 118:5381–5392. doi:10.1242/jcs.02652

Zhang, L., and A.S. Maddox. 2010. Anillin. *Curr. Biol.* 20:R135–R136. doi:10.1016/j.cub.2009.12.017

Zhao, W.M., and G. Fang. 2005. MgcRacGAP controls the assembly of the contractile ring and the initiation of cytokinesis. *Proc. Natl. Acad. Sci. USA*. 102:13158–13163. doi:10.1073/pnas.0504145102

Zhou, M., and Y.L. Wang. 2008. Distinct pathways for the early recruitment of myosin II and actin to the cytokinetic furrow. *Mol. Biol. Cell*. 19:318–326. doi:10.1091/mbc.E07-08-0783

Zhu, C., E. Bossy-Wetzel, and W. Jiang. 2005. Recruitment of MKLP1 to the spindle midzone/midbody by INCENP is essential for midbody formation and completion of cytokinesis in human cells. *Biochem. J.* 389:373–381. doi:10.1042/BJ20050097